Dalton Transactions

Accepted Manuscript

ROYAL SOCIETY OF CHEMISTRY

www.rsc.org/dalton

Spatial distribution of phases during gradual magnetostructural transitions in copper(II)-nitroxide based molecular magnets

Matvey V. Fedin,[a,b] Sergey L. Veber, [a,b] Elena G. Bagryanskaya,[b,c] Galina V. Romanenko,[a] Victor I. Ovcharenko[a]

[a]*International Tomography Center SB RAS, 630090, Novosibirsk, Russia*

[b]*Novosibirsk State University, 630090, Novosibirsk, Russia*

[c]*N. N. Vorozhtsov Novosibirsk Institute of Organic Chemistry SB RAS, 630090, Novosibirsk, Russia*

Abstract

Copper(II)-nitroxide based molecular magnets $Cu(hfac)_2L^R$ exhibit thermally-induced transitions between high- and low-temperature (HT/LT) magnetostructural states. In this work we report the first study on spatial distribution of HT/LT phases during gradual transitions in these compounds. We explore the possibility of domains formation at intermediate temperatures that was never addressed before. For this purpose, we reexamine the available electron paramagnetic resonance (EPR) and X-ray diffraction data, and perform numerical calculations of EPR spectra for different models of exchange-coupled networks. Thorough analysis shows that during gradual transitions molecular magnets $Cu(hfac)_2L^R$ represent solid solutions of disordered HT and LT phases, and the formation of single-phase domains larger than a few nanometers in size is unlikely.

Introduction

Design of molecular switches is an attractive field of fundamental research with promising perspective for future applications in nanosensing, data storage etc. In particular, a lot of studies have been focused on spin crossover (SCO) and related phenomena often found in transition metal complexes.[1-7] Many topics of interest have been extensively investigated, including influence of chemical structure on SCO, influence of external stimuli such as pressure, light etc., relaxation behavior between phases, nature of cooperativity, theoretical models of SCO phenomena, etc.

Copper(II)-nitroxide based molecular magnets exhibit magnetic phenomena in many aspects similar to SCO.[8,9] Although spin state of copper(II) cannot be changed, the total spin state of exchange-coupled copper(II)-nitroxide cluster can. These complexes contain either spin triads nitroxide-copper(II)-nitroxide or spin pairs copper(II)-nitroxide and undergo temperature-induced magnetostructural rearrangements of Jahn-Teller nature. They are often called "breathing crystals" due to the large and reversible changes of unit cell volume occurring upon magnetostructural transition. The elongated (Jahn-Teller) axes of coordination octahedra CuO_6 (for triads) or CuO_5N (for pairs) occupy different directions at high and low temperatures (HT/LT), creating two distinct structural states characterized by two different exchange couplings between copper(II) and nitroxide spins (J). Typically, HT structure corresponds to nitroxide ligands in axial coordination positions, resulting in weak ferromagnetic exchange J (so-called weakly-coupled spin state, WS). Instead, LT structure corresponds to nitroxide ligands in equatorial coordination positions, where J is strong antiferromagnetic (strongly-coupled spin state, SS). Stimuli-induced switching between these two states of breathing crystals is of great interest, and various related phenomena have been observed in other systems as well.[10-20]

The family of breathing crystals $Cu(hfac)_2L^R$ has dramatically expanded over last decade and presently includes more than 50 compounds, most of which were extensively characterized by X-ray diffraction (XRD), SQUID magnetometry, electron paramagnetic resonance (EPR), and some recently by optical spectroscopies.[8,9,21-34] Temperature dependence of the effective magnetic moment ($\mu_{eff}(T)$) strongly varies from compound to compound: abrupt or gradual transitions with one to three steps of different amplitude may be observed. In general, abrupt transitions are associated with high cooperativity and concerted switching of all clusters from one phase to another. At the same time, nature and molecular-level structure during gradual transitions is much less understood.

First possible explanation of gradual $\mu_{eff}(T)$ dependence observed in many breathing crystals relies on the interplay of gradually changing geometry of coordination octahedra in conjunction

with changes of exchange couplings and corresponding populations of spin levels. In principle, XRD data support this idea, since they also report gradual structural changes with temperature. However, if one phase is disordered inside the other one (solid solution), XRD is likely to report a spatially-averaged structure being a weighted combination of the two phases. Thus, second possible explanation has to be considered, namely that gradual transition in breathing crystals results from consequent switching of exchange-coupled clusters from one state to another.

EPR of breathing crystals provides an excellent opportunity to distinguish between SS and WS states (LT/HT geometries), because the corresponding spectra are distinctly different.[9] Therefore, it seems that EPR data should be decisive for the two above explanations. However, it was found that relatively weak intercluster exchange couplings (J_{inter}~1-10 cm^{-1}) between neighboring clusters couple them into an infinite chain and lead again to the averaging of signals of SS and WS states at intermediate temperatures.[26] Conclusive evidence was recently found by FTIR spectroscopy, which is sensitive to the structural changes, but not sensitive to magnetic interactions.[34] Studying the breathing crystal with gradual transition, we observed gradual replacement of one phase by another and no signs of intermediate phases. This clearly shows that the second explanation is valid: the two phases coexist during gradual transitions in breathing crystals, and temperature-dependent ratio of these phases results in the observed gradual changes in SQUID, XRD and EPR. Recent quantum-chemical studies provided an additional evidence for this conclusion.[35]

Having understood this, the next interesting question is whether or not magnetostructural domains exist at the intermediate temperatures. A number of studies addressed this topic for SCO compounds previously,[36-45] and unveiling similar information for breathing crystals would be a topical task. In general, gradual transitions imply low cooperativity, and low cooperativity implies no domains formed, since domains ultimately result from cooperative interactions. However, (i) cooperativity in breathing crystals is still an unexplored field due to the pronounced synthetic difficulties in creation of magnetically-diluted analogues, and (ii) the occurrence of magnetic anomalies on the scale of exchange cluster (not a single ion) supposes much higher sensitivity of breathing crystals to the subtle cooperative interactions. The latter was indirectly confirmed by a very high sensitivity of breathing crystals to such external influences as pressure,[46] embedding in polymer matrix,[32] and even severe grinding.

Thus, the question on possible domain structures vs. purely solid solution of two phases during gradual transitions in breathing crystals needs further investigation. In this work we perform numerical simulation of previously obtained high-field EPR spectra[25] assuming domain structures of various sizes. Using this approach, we set upper limit for the domain size that allows fair

agreement with experimental EPR data. We also reexamine XRD data at intermediate temperatures yielding information on possible domain formation. Combination of these analyses allowed us to conclude on the spatial distribution of phases in the studied compounds.

Results and Discussion

Analysis of EPR data

As was already mentioned above, EPR spectra corresponding to the two magnetostructural states of spin triads ({HT geometry, WS state} and {LT geometry, SS state}) are distinctly different.[9] WS state is characterized by g>2 values, whereas SS state has g<2. We restrict ourselves here to spin triads only and do not consider spin pairs, because available experimental data for the former type of clusters is much more abundant.[8,9]

Why can SS and WS states in breathing crystals become indistinguishable by EPR? The reason is the interplay of intercluster exchange interaction J_{inter} and temporal resolution of EPR traced back to the detection using oscillating (typically ~9-300 GHz) microwave magnetic field. If two clusters in different states are coupled by J_{inter}, electron is delocalized between these two clusters with characteristic hopping frequency being roughly $f \sim J_{inter}$.[47] Assume that the two individual lines of SS and WS states are separated by static magnetic field $\Delta B \equiv \Delta\nu/\gamma_e$ (where γ_e is the gyromagnetic ratio), and electron hops between these two states. The shape of the overall EPR spectrum will strongly depend on the ratio between $\Delta\nu$ and f. In the limiting case $\Delta\nu << f$, the two individual lines coalesce into a single EPR line with averaged spectral characteristics.[48] If we extend our consideration to the large network of exchange-coupled clusters, hyperfine and dipolar-type interactions may become completely averaged due to the electron hopping, and so-called exchange narrowing is observed. In the opposite limiting case $\Delta\nu >> f$, the influence of exchange can be neglected and two individual EPR lines of SS and WS states may be resolved. Since $\Delta\nu$ depends on ΔB (and thus on the operating frequency of EPR spectrometer ν_{mw}), while f is purely a property of spin system, variation of ν_{mw} changes the ratio between $\Delta\nu$ and f, being a useful experimental approach in many situations.

Consider now the realistic model of breathing crystals: an infinite linear chain of clusters coupled by intercluster exchange J_{inter} (Fig.1). Exactly this magnetic motif has been established by means of EPR and quantum chemistry studies.[26] Depending on the magnitude of J_{inter} (that for simplicity is assumed isotropic), the rate of spin diffusion (i.e. electron propagation/hopping) along the chain will take finite values. If continuous sequences of clusters in the same spin state (that we will call “domains”) will be long enough, a very strong J_{inter} will be necessary to fully average EPR

signals of neighboring domains of different phase. This is clearly understood because clusters in the center of big domain will have nearly zero interaction with clusters of the neighboring domain. Contrary to that, if clusters in different states are homogeneously mixed, so that there are no large domains of the same phase, much smaller J_{inter} couplings will efficiently exchange-narrow the EPR signals of two phases. Thus, clearly, for linear chains of exchange-coupled clusters the shape of the EPR spectrum will be sensitive to the ratio between the domain size and J_{inter} value, and this is exactly the property that we would like to exploit for the estimation of domain sizes in breathing crystals.

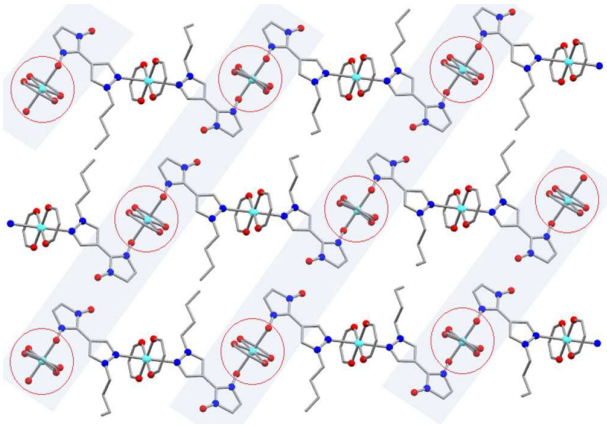

Figure 1. Typical structure of breathing crystals exemplified using complex $Cu(hfac)_2L^{Bu}\cdot C_7H_{16}$ at 150 K (WS state). Spin triads are circled, magnetic chains spreading across the structural polymer chains through NO…ON contacts are highlighted in grey. Color code: Cu – light blue, O – red, N – blue, C – grey.

We model infinite chain of coupled spin triads by 16- or 32-membered rings, where each triad has g-factor g_{SS} or g_{WS} depending on its state (Fig. 2). Previous studies assume that such rings model infinite chains very well,[49,26] and, in addition, we have found the identical results obtained for 16- and 32-membered rings in this study. Each triad is connected by J_{inter} only with the two of its neighbors in the chain (ring). In order to account for EPR detection and describe exchange narrowing, we consider the magnetization vector of each cluster (triad) M^i and use the system of 32 modified Bloch equations for the complex variables $G^i = M_x^i - iM_y^i$ (i=1 to 32; (i+1)=33 refers to 1, (i-1)=0 refers to 32):

$$\frac{dG^i}{dt} = -\frac{G^i}{T_2^i} + i\Delta\omega^i G^i - i\omega_1 M_0^i - \frac{G^i}{\tau_{i\to i+1}} - \frac{G^i}{\tau_{i\to i\text{-}1}} + \frac{G^{i+1}}{\tau_{i+1\to i}} + \frac{G^{i\text{-}1}}{\tau_{i\text{-}1\to i}} \qquad (1)$$

where $M_{x,y,0}^i$ correspond to x, y and equilibrium components of magnetization vector of the i-th cluster, T_2^i is the transverse relaxation time of i-th cluster in the absence of intercluster exchange, $\Delta\omega^i$ is the corresponding resonance offset, ω_1 is the microwave field amplitude, $\tau_{i\to j}$ is the electron

hopping rate from *i*-th to *j*-th cluster. Since we seek a stationary solution of this system, $dG^i/dt = 0$; the absorption lineshape is then obtained as usual by taking $M_y = -\mathrm{Im}\left(\sum_{i=1-32} G^i\right)$. For simplicity we assume the T_2^i and $\tau_{i\to j}$ values equal for all *i,j*.

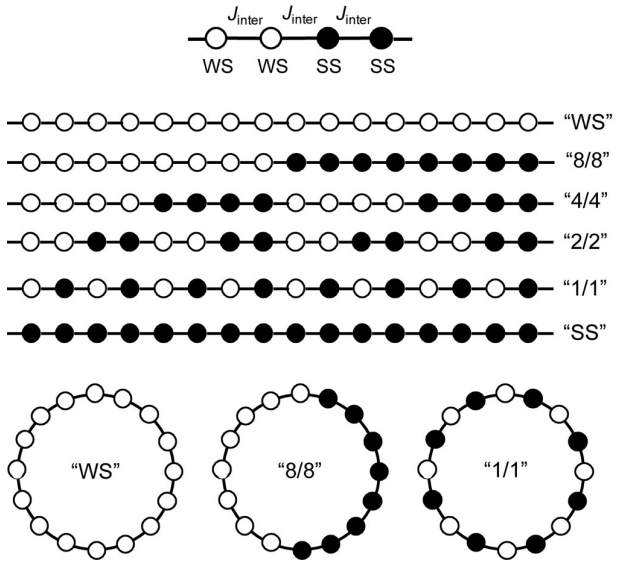

Figure 2. Models of exchange-coupled chains of spin triads in breathing crystals. Filled circles correspond to spin triads in SS state, open circles for spin triads in WS state, exchange coupling between any neighboring triads is taken as J_{inter}. 16-membered "rings" in the bottom (and 32-membered analogues which are not shown) were assumed to be good models of corresponding infinite polymer chains.

Figure 3 shows the results of model calculations for the "1/1" model (regular alternation of clusters in WS and SS states with overall equal amount of each state) for different values of intercluster exchange J_{inter}. As will be obvious below, the spectroscopic parameters considered in this calculation are typical for breathing crystals. The obtained trends perfectly agree with qualitative expectations. At smallest values of J_{inter}=0.01 cm^{-1} we observe two resolved EPR lines that are relatively narrow being mainly determined by T_2 relaxation time. At higher values of J_{inter} the two lines start to broaden and coalesce at J_{inter}>0.5 cm^{-1}; at even higher values of J_{inter} the coalesced line exchange-narrows. All these observations are typical for exchange narrowing (or motional narrowing) observed in EPR or NMR experiments.[48]

Next, we investigate the influence of domain size (where domain means the sequence of clusters in the same state) on EPR spectrum at fixed J_{inter} and compare the results with previously reported experimental data.[25] We focus on two representatives of the breathing crystals family, $Cu(hfac)_2L^{Bu}\cdot 0.5C_8H_{18}$ (where C_8H_{18} is *n*-octane) and $Cu(hfac)_2L^{Pr}$, that have been previously investigated by EPR in broad frequency range 34-244 GHz.[25] In addition, quantum chemical calculations of intercluster (interchain) exchange couplings are also available for these two

compounds: they equal to $|J_{inter}|$=9.55 cm^{-1} ($Cu(hfac)_2L^{Bu}\cdot 0.5C_8H_{18}$) and $|J_{inter}|$=0.33 cm^{-1} ($Cu(hfac)_2L^{Pr}$) in SS state at UB3LYP/6-31+G* level and do not change much (only by a factor of ~2) with temperature.[26,35]

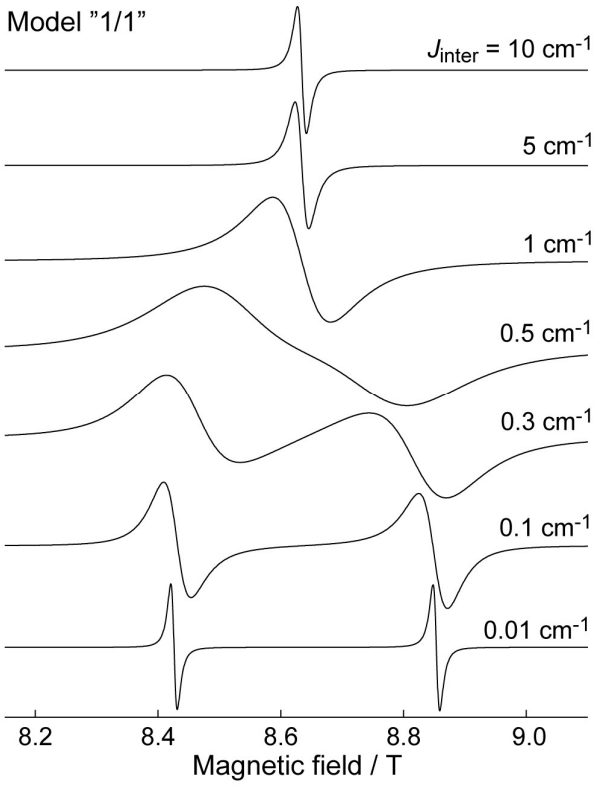

Figure 3. Calculated EPR spectra of 32-membered ring with regularly alternating clusters in WS and SS state (model "1/1") vs. value of intercluster exchange coupling J_{inter}. Model parameters used: microwave frequency ν_{mw}=244 GHz; g-factors of WS and SS states g_{WS}=2.07, g_{SS}=1.97; T_2=1 ns; $\omega_1=10^4$ s^{-1}; values of J_{inter} are indicated on the plot. All spectra are normalized.

Figure 4a shows experimental EPR data for $Cu(hfac)_2L^{Bu}\cdot 0.5C_8H_{18}$ obtained previously at 244 GHz.[25] This compound exhibits gradual magnetostructural transition between ~90 K (SS state) and ~180 K (WS state). In Fig.4a (and Figs. 5a, 6a below) we show experimental EPR spectra of spin triads only. Single crystal (arbitrary) orientations in Ref.25 were adjusted to resolve completely the signals of spin triads and signals of one-spin CuN_4O_2 units (that appear at lower magnetic fields) at any temperature. Remarkably, we observed single EPR line of spin triad at all frequencies up to 244 GHz and at any temperature.[25] The shape of EPR line experienced pronounced changes, and the position gradually moved from that of WS to SS state as temperature changed; however, no resolved EPR lines of WS/SS states were detected. This means, that if the two states coexist at intermediate temperatures, the averaging due to J_{inter} should be very efficient.

For simplicity of modeling, we restrict calculations to the particular situation when the number of WS states equals to the number of SS states, i.e. the transition is just 50% complete. For $Cu(hfac)_2L^{Bu}\cdot 0.5C_8H_{18}$ this corresponds approximately to 120 K, because $\mu_{eff}^2(WS) \approx 3\mu_{eff}^2(SS)$. Integral intensity of EPR lines in WS and SS states also differs by a factor of 3; however, without loss of generality and with the gain of visualization, the coalescence regime can be studied for two lines of the same integral intensity.

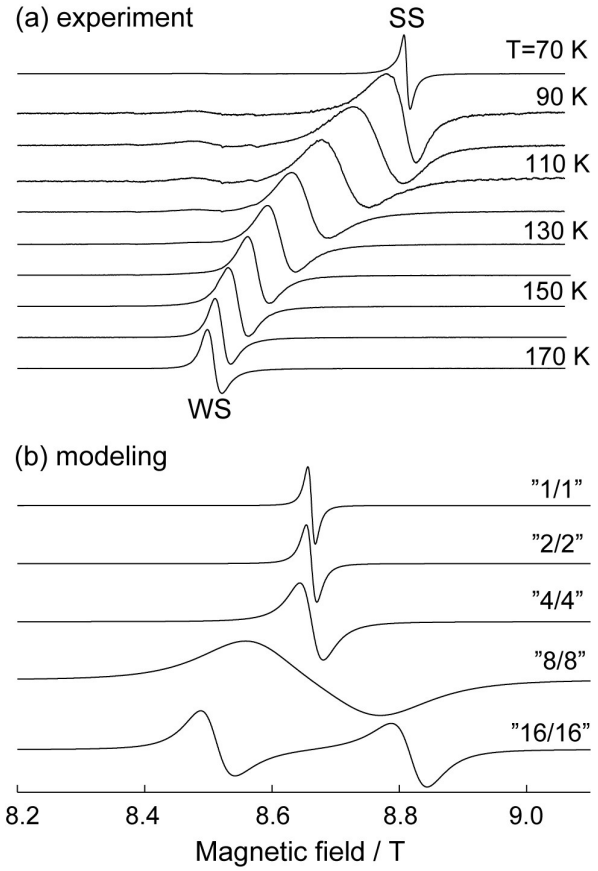

Figure 4. (a) Experimental EPR spectra of $Cu(hfac)_2L^{Bu}\cdot 0.5C_8H_{18}$ (single crystal) obtained at 244 GHz (data published previously in ref.25). All spectra are normalized. The indicated range of magnetic field corresponds to spin triads (CuO_6 units) only, whereas EPR signals of CuO_4N_2 units appear at lower magnetic fields for chosen crystal orientation and are not shown (for full EPR spectra see ref.25) (b) Calculated EPR spectra of 32-membered ring for different models of WS/SS spatial distribution (indicated on the plot). In all cases the amounts of WS and SS states were equal and J_{inter}=10 cm^{-1}. Other parameters used: microwave frequency ν_{mw}=244 GHz; g-factors of WS and SS states g_{WS}=2.053, g_{SS}=1.974; T_2=1 ns; $\omega_l=10^4$ s^{-1}. All spectra are normalized.

Figure 4b shows calculated spectra of 32-membered ring in five models corresponding to the continuous sequences of WS/SS states being 1 ("1/1"), 2 ("2/2"), 4 ("4/4"), 8 ("8/8") and 16 ("16/16") (see Fig. 2). In all cases the value of J_{inter}=10 cm^{-1} was used, in agreement with previously reported value J_{inter} = 9.55 cm^{-1}.[26] Indeed, a single exchange-narrowed EPR line is observed in

"1/1", "2/2" and "4/4" models; however, starting from about 8 clusters of the same phase in a row the two lines become resolved. This reflects that for the same-phase domains of more than 8 clusters J_{inter} = 10 cm^{-1} is not large enough to cause observation of single exchange-narrowed line. Thus, model calculation restricts the domain size in $Cu(hfac)_2L^{Bu}\cdot 0.5C_8H_{18}$ at a level of ~8 clusters. One may argue that J_{inter} value calculated quantum-chemically is not accurate enough; however, the drop of $\mu_{eff}(T)$ dependence at T<20 K agrees very well with this value.[26] Another objection can arise from the accuracy of estimation of the electron hopping rate to be $f \sim J_{inter} \sim 1/\tau$. This is indeed a crude estimate, and to validate results we perform model calculations for the second compound $Cu(hfac)_2L^{Pr}$ at two microwave bands.

Breathing crystal $Cu(hfac)_2L^{Pr}$ develops gradual magnetostructural transition between ~90 K (SS state) and ~250 K (WS state), with equal concentration of two states around 170-180 K. $Cu(hfac)_2L^{Pr}$ has much smaller value of $J_{inter} \sim 0.3$ cm^{-1} compared to $Cu(hfac)_2L^{Bu}\cdot 0.5C_8H_{18}$. In agreement with that, EPR spectra at 244 GHz demonstrate clearly resolved signals of SS and WS states at intermediate temperatures. Indeed, using $J_{inter} \sim 0.3$ cm^{-1} we easily obtain two resolved EPR lines even in "1/1" model (Fig.5b). Remarkably, the apparent linewidth in "1/1" model is very similar to that observed experimentally at 150-215 K (Fig.5a). Models "4/4"-"16/16" give much narrower spectra, close to those of pure SS state (90 K) or pure WS state (260 K). Thus, judging from linewidth, "1/1" model is again most adequate to account for experimental observations.

Furthermore, calculations for $Cu(hfac)_2L^{Pr}$ can also be done at Q-band (34 GHz) mw frequency. At this relatively low frequency resolved lines of WS and SS states are not observed; instead, single EPR line moving with temperature is found (Fig. 6a), quite similar to the data for $Cu(hfac)_2L^{Bu}\cdot 0.5C_8H_{18}$ at 244 GHz (Fig. 4a). Using $J_{inter} \sim 0.3$ cm^{-1} we obtain that only "1/1" and "2/2" models result in single exchange-narrowed EPR line, whereas larger sequences of clusters in the same phase ("4/4"-"16/16" models) result in resolved structure that is not observed experimentally. Thus, similar to the first compound, EPR data on $Cu(hfac)_2L^{Pr}$ presumes that only small domains (<4 clusters in size) can hypothetically be formed in course of gradual magnetostructural transition.

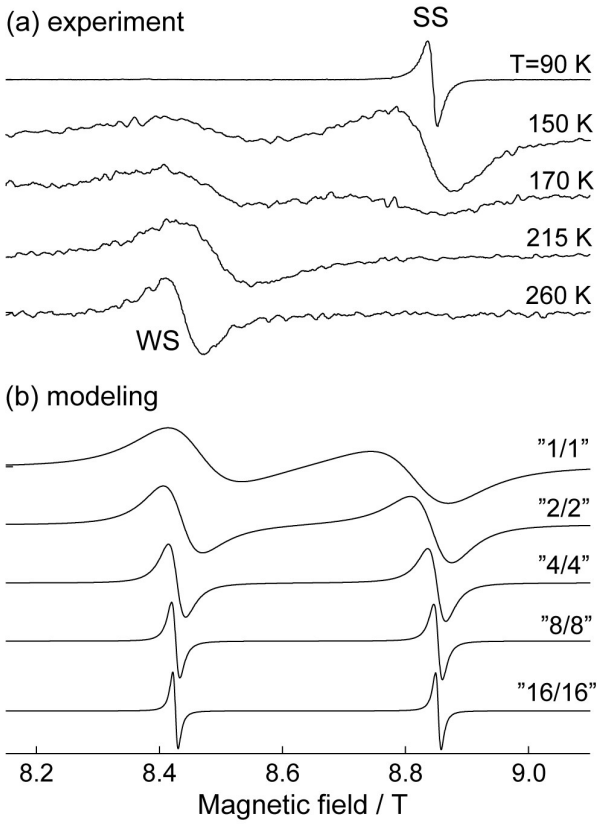

Figure 5. (a) Experimental EPR spectra of $Cu(hfac)_2L^{Pr}$ (single crystal) obtained at 244 GHz (data published previously in ref.25). All spectra are normalized. The indicated range of magnetic field corresponds to spin triads (CuO_6 units) only, whereas EPR signals of CuO_4N_2 units appear at lower magnetic fields for chosen crystal orientation and are not shown (for full EPR spectra see ref.25) (b) Calculated EPR spectra of 32-membered ring for different models of WS/SS spatial distribution (indicated on the plot). In all cases the amounts of WS and SS states were equal and J_{inter}=0.3 cm^{-1}. Other parameters used: microwave frequency ν_{mw}=244 GHz; g-factors of WS and SS states g_{WS}=2.07, g_{SS}=1.97; T_2=1 ns; $\omega_1=10^4$ s^{-1}. All spectra are normalized.

Note that all considerations above were done in the model where a particular cluster switches from one state to another only once in course of the transition and statically resides in SS or WS state in the rest of the time. However, Jahn-Teller (JT) nature of breathing crystals does not exclude that each cluster might oscillate between two states (WS or SS having different JT axis) with the frequency on the order of GHz, so that the ratio of WS and SS states at particular temperature (e.g. measured by FTIR) is a statistical number.[9] Similar manifestations of dynamic JT effect and vibronic coupling are well known for copper(II) complexes,[50-54] and the possibility of dynamic JT behavior in breathing crystals could not be disproved by any experimental technique so far. Note, however, that such "dynamic equilibrium" between SS and WS phases in course of gradual magnetostructural transition is in principle inconsistent with the existence of domains of separate phases. Thus, whether equilibrium between different phases is dynamic or static, the restrictions for the domains size obtained by our modeling above remain valid.

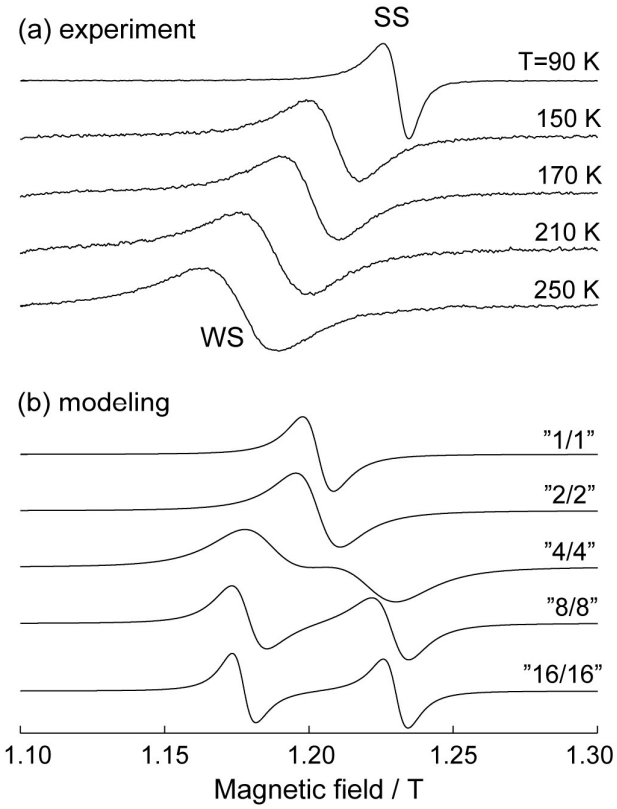

Figure 6. (a) Experimental EPR spectra of $Cu(hfac)_2L^{Pr}$ (single crystal) obtained at 34 GHz (data published previously in ref.25). All spectra are normalized. The indicated range of magnetic field corresponds to spin triads (CuO_6 units) only, whereas EPR signals of CuO_4N_2 units appear at lower magnetic fields for chosen crystal orientation and are not shown (for full EPR spectra see ref.25) (b) Calculated EPR spectra of 32-membered ring for different models of WS/SS spatial distribution (indicated on the plot). In all cases the amounts of WS and SS states were equal and J_{inter}=0.3 cm^{-1}. Other parameters used: microwave frequency ν_{mw}=34 GHz; g-factors of WS and SS states g_{WS}=2.065, g_{SS}=1.975; T_2=1 ns; $\omega_1=10^4$ s^{-1}. All spectra are normalized.

Analysis of XRD data

Although crystal structures obtained by XRD analysis generally provide spatial averages over the crystal volume, one anticipates that such parameters of solved structure as symmetry, R-factor and mosaicity[55-57] can indirectly inform on the possibility of domain formation in biphasic compounds. E.g., if large enough domains are formed, additional symmetry constrains might be required to solve the structure. Contrary, if two phases are homogeneously distributed in the crystal, the long-range order should be found and the percentage of symmetry breakings is expected to be low. At least qualitatively, such reconsideration of crystal data can confirm or disprove the conclusions made solely on the basis of EPR above.

The detailed analysis of crystal structure of $Cu(hfac)_2L^{Pr}$ (single crystal, see Electronic Supplementary Information (ESI)) reveals abrupt symmetry change at ~220 K. Base-centered cell

(monoclinic space group $C2/c$) is found at T=290-225 K with insignificant percentage of this symmetry breakings <3.1% (Table S1 of ESI), indicating the presence of long-range order and confirming statistically homogeneous distribution of WS phase with the small admixture of SS phase. However, the processing of data collected at 220 K assuming space group $C2/c$ yields >50% of breakings of base-centered unit cell (i.e. reflections with $h+k \neq 2n$). At the same time, assuming space group $P2_1/n$ that is an isomorphous sub-group of $C2/c$, we find the percentage of symmetry breakings as small as <3.1%. The difference in Cu atoms positions in space groups $C2/c$ and $P2_1/n$ is ascribed to the loss of centrosymmetry in coordination units $\{CuO_6\}$ (Cu(1) in Fig. 7a) at 220 K, whereas the coordination units $\{CuO_4N_2\}$ are always centrosymmetrical (one crystallographically-independent unit of $C2/c$ symmetry (Cu(2) in Fig. 7a) and two units of $P2_1/n$ symmetry (Cu(1) and Cu(3) in Fig. 7b)). Note that even though the $\{CuO_6\}$ unit is not centrosymmetrical, its two Cu-O_{NO} distances are virtually the same at 220 K, as well as at lower temperatures.

Thus, three simultaneous observations are made in the temperature region of mixed phases (220 K), namely (i) crystal symmetry changes compared to the pure phases, (ii) low percentage of symmetry breakings (<3.1%) implies long-range order and a good quality of the sample, and (iii) the two Cu-O_{NO} distances in $\{CuO_6\}$ units are similar at T=220 K and below. Altogether, these observations are strongly favorable for the "1/1" model of homogeneously distributed units in WS and SS states in the crystal. At least XRD data do not point out to a multiple increase of any parameter of the unit cell, which would be expected for large enough domains.

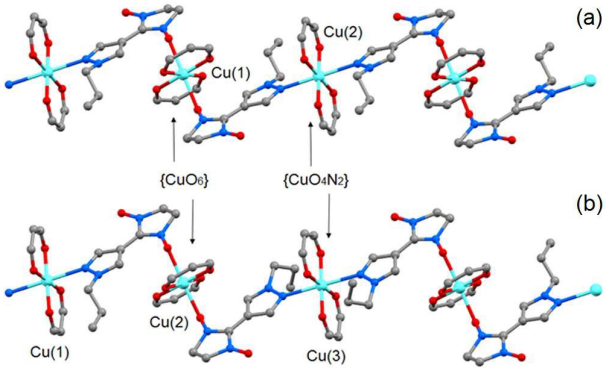

Figure 7. (a) Polymer chain in $Cu(hfac)_2L^{Pr}$ at 220 K in $C2/c$ space group (n-Pr substituent is disordered on three positions (0.4/0.4/0.2) and only one position is shown. (b) Polymer chain in $Cu(hfac)_2L^{Pr}$ at 220 K in $P2_1/n$ space group. Color code: Cu – light blue, O – red, N – blue, C – grey.

Conclusions

In this work we have revisited previously obtained experimental EPR data[25] on breathing crystals $Cu(hfac)_2L^R$; we have analyzed these data using numerical calculations in order to obtain constraints for the size of domains potentially formed during gradual magnetostructural transitions.

Our analysis clearly shows that during gradual transitions molecular magnets $Cu(hfac)_2L^R$ represent solid solutions of two disordered phases, and formation of single-phase domains larger than 4-8 clusters is hardly possible. Having the cluster size of ~1.3 nm, we set the upper limit of the domain size as ~5-10 nm, whereas the real size is likely to be smaller. Additional XRD analyses support these EPR-based findings. Note that apart from targeted application to particular family of compounds done in this work, the proposed methodology is generally applicable for studying spatial distribution of different types of paramagnetic centers in solids. To the best of our knowledge, such approach has been demonstrated by us here for the first time.

Understanding the spatial distribution of two phases in switchable molecular magnets $Cu(hfac)_2L^R$ is highly important from both fundamental and applied sides. In particular, the present study shows that magnetic properties of clusters in two different states, namely individual magnetic moments and exchange couplings, are averaged on the scale of a few nanometers. Unless a really single-ion/cluster property is targeted, one generally can operate with the average values, as was previously done in numerous EPR studies.[9] In addition, this implies that nanocrystals of a few nm in size should reflect the physical properties of the big crystals, aiding their prospective preparation on surfaces for prototyping molecular spin devices. More experimental work is certainly required to downscale the crystals of $Cu(hfac)_2L^R$ family to nanometers and study their properties, and the present work sustains this topical direction of future research.

Acknowledgement

This work was supported by the RF Federal Agency for Scientific Organizations, RFBR (No.14-03-00224, 15-03-07640 and 14-03-00517) and RF President's Grants (MD-276.2014.3, MK-3241.2014.3).

References

[1] P. Gutlich, H. A. Goodwin (Eds.), Spin Crossover in Transition Metal Compounds, Topics in Current Chemistry, vol. I–III, Springer-Verlag, Berlin/Heidelberg/NewYork, 2004, pp. 233–235.

[2] M. A. Halcrow (Ed.), Spin-Crossover Materials: Properties and Applications, firsted., John Wiley & Sons, Ltd., Oxford, UK, 2013.

[3] A. Bousseksou, G. Molnar, L. Salmon, W. Nicolazzi, *Chem. Soc. Rev.*, 2011, **40**, 3313-3335.

[4] J. A. Real, A. B. Gaspar, M. C. Munoz, *Dalton Trans*., 2005, 2062-2079.

[5] G. S. Matouzenko, M. Perrin, B. Le Guennic, C. Genre, G. Molnar, A. Bousseksou, S. A. Borshch, *Dalton Trans*., 2007, 934-942.

[6] S. Brooker, J. A. Kitchen, *Dalton Trans.*, 2009, 7331-7340.

[7] P. Gamez, J. S. Costa, M. Quesada, G. Aromi, *Dalton Trans*., 2009, 7845-7853.

[8] V. I. Ovcharenko, E.G. Bagryanskaya, in: M.A. Halcrow (Ed.), Spin-Crossover Materials: Properties and Applications, first ed., John Wiley & Sons, Ltd., 2013, pp. 239–280.

[9] M. V. Fedin, S. L. Veber, E. G. Bagryanskaya, V. I. Ovcharenko, *Coord. Chem. Rev.,* 2015, **289-290**, 341-356.

[10] A. Caneschi, P. Chiesi, L. David, F. Ferraro, D. Gatteschi, R. Sessoli, *Inorg. Chem.,* 1993, **32**, 1445-1453.

[11] F. Lanfranc de Panthou, E. Belorizky, R. Calemczuk, D. Luneau, C. Marcenat, E. Ressouche, P. Turek, P. Rey, *J. Amer. Chem. Soc.*, 1995, **117**, 11247-11253.

[12] K. Inoue, F. Iwahori, H. Iwamura, *Chem. Lett.,* 1998, 737-738.

[13] F. Iwahori, K. Inoue, H. Iwamura, *Mol. Cryst. Liq. Cryst.*, 1999, **334**, 533-538.

[14] M. Baskett, P. M. Lahti, A. Paduan-Filho, N. F. Oliveira, *Inorg. Chem.,* 2005, **44**, 6725-6735.

[15] M. Baskett, A. Paduan-Filho, N. F. Oliveira, A. Chandrasekaran, J. T. Mague, P. M. Lahti, *Inorg. Chem.*, 2011, **50**, 5060-5074.

[16] R. A. Allão Cassaro, M. Baskett, P. M. Lahti, *Polyhedron*, 2013, **64**, 231-237.

[17] C. Hirel, L. Li, P. Brough, K. Vostrikova, J. Pecaut, B. Mehdaoui, M. Bernard, P. Turek, P. Rey, *Inorg. Chem.*, 2007, **46**, 7545-7552.

[18] F. Setifi, S. Benmansour, M. Marchivie, G. Dupouy, S. Triki, J. Sala-Pala, J. Y. Salaun, C. J. Gomez-Garcia, S. Pillet, C. Lecomte, E. Ruiz, *Inorg. Chem.,* 2009, **48**, 1269-1271.

[19] A. Okazawa, D. Hashizume, T. Ishida, *J. Amer. Chem. Soc.,* 2010, **132**, 11516-11524.

[20] A. Okazawa, T. Ishida, *Inorg. Chem.*, 2010, **49**, 10144-10147.

[21] V. I. Ovcharenko, S.V. Fokin, G.V. Romanenko, Yu.G. Shvedenkov, V.N. Ikorskii, E.V. Tretyakov, S.F. Vasilevskii, *J. Struct. Chem*., 2002, **43**, 153-167.

[22] M. Fedin, S. Veber, I. Gromov, K. Maryunina, S. Fokin, G. Romanenko, R. Sagdeev,V. Ovcharenko, E. Bagryanskaya, *Inorg. Chem*., 2007, **46**, 11405-11415.

[23] S. L. Veber, M. V. Fedin, A. I. Potapov, K. Y. Maryunina, G. V. Romanenko, R. Z. Sagdeev, V. I. Ovcharenko, D. Goldfarb, E. G. Bagryanskaya, *J. Amer. Chem. Soc.*, 2008, **130**, 2444-2445.

[24] M. Fedin, V. Ovcharenko, R. Sagdeev, E. Reijerse, W. Lubitz, E. Bagryanskaya, *Angew. Chem. Int. Ed*., 2008, **47**, 6897-6899.

[25] M. V. Fedin, S. L. Veber, G. V. Romanenko, V. I. Ovcharenko, R. Z. Sagdeev, G. Klihm, E. Reijerse, W. Lubitz, E. G. Bagryanskaya, *Phys. Chem. Chem. Phys*., 2009, **11**, 6654-6663.

[26] M. V. Fedin, S. L. Veber, K. Y. Maryunina, G. V. Romanenko, E. A. Suturina, N. P. Gritsan, R. Z. Sagdeev, V. I. Ovcharenko, E. G. Bagryanskaya, *J. Amer. Chem. Soc*., 2010, **132**, 13886-13891.

[27] S. L. Veber, M. V. Fedin, K. Y. Maryunina, A. Potapov, D. Goldfarb, E. Reijerse, W. Lubitz, R. Z. Sagdeev, V. I. Ovcharenko, E. G. Bagryanskaya, *Inorg. Chem*., 2011, **50**, 10204-10212.

[28] G. V. Romanenko, K. Y. Maryunina, A. S. Bogomyakov, R. Z. Sagdeev, V. I. Ovcharenko, *Inorg. Chem*., 2011, **50**, 6597-6609.

[29] E. V. Tretyakov, S. E. Tolstikov, A. O. Suvorova, A. V. Polushkin, G. V. Romanenko, A. S. Bogomyakov, S. L. Veber, M. V. Fedin, D. V. Stass, E. Reijerse, W. Lubitz, E. M. Zueva, V. I. Ovcharenko, *Inorg. Chem*., 2012, **51**, 9385-9394.

[30] M. V. Fedin, K. Y. Maryunina, R. Z. Sagdeev, V. I. Ovcharenko, E. G. Bagryanskaya, *Inorg. Chem*., 2012, **51**, 709-717.

[31] M. V. Fedin, E. G. Bagryanskaya, H. Matsuoka, S. Yamauchi, S. L. Veber, K. Y. Maryunina, E. V. Tretyakov, V. I. Ovcharenko, R. Z. Sagdeev, *J. Amer. Chem. Soc*., 2012, **134**, 16319-16326.

[32] I. Yu. Barskaya, E. V. Tretyakov, R. Z. Sagdeev, V. I. Ovcharenko, E. G. Bagryanskaya, K. Yu. Maryunina, T. Takui, K. Sato, M. V. Fedin, *J. Amer. Chem. Soc*., 2014, **136**, 10132-10138.

[33] W. Kaszub, A. Marino, M. Lorenc, E. Collet, E. G. Bagryanskaya, E. V. Tretyakov,V. I. Ovcharenko, M. V. Fedin, *Angew. Chem. Int. Ed.,* 2014, **53**, 10636-10640.

[34] S. L. Veber, E. A. Suturina, M. V. Fedin, K. N. Boldyrev, K. Y. Maryunina, R. Z. Sagdeev, V. I. Ovcharenko, N. P. Gritsan, E G. Bagryanskaya, *Inorg. Chem*., 2015, **54**, 3446-3455.

[35] J. Jung, B. Le Guennic, M. V. Fedin, V. I. Ovcharenko, C. J. Calzado, *Inorg. Chem*. 2015, **54**, 6891-6899.

[36] W. Nicolazzi, S. Pillet, C. Lecomte, *Phys. Rev. B*, 2008, **78**, 174401.

[37] S. Bonnet, M. A. Siegler, J. Sanchez Costa, G. Molnar, A. Bousseksou, A. L. Spek, P. Gameza, J. Reedijk, *Chem. Commun.*, 2008, 5619-5621.

[38] C. Enachescu, L. Stoleriu, A. Stancu, A. Hauser. *Phys. Rev. Lett*., 2009, **102**, 257204.

[39] C. Chong, F. Varret, K. Boukheddaden, *Phys. Rev. B*, 2010, **81**, 014104.

[40] M. Nishino, C. Enachescu, S. Miyashita, K. Boukheddaden, F. Varret, *Phys. Rev. B*, 2010, **82**, 020409.

[41] A. Slimani, F. Varret, K. Boukheddaden, C. Chong, H. Mishra, J. Haasnoot, S. Pillet, *Phys. Rev. B*, 2011, **84**, 094442.

[42] W. Nicolazzi, S. Pillet, *Phys. Rev. B*, 2012, **85**, 094101.

[43] W. Nicolazzi1, J. Pavlik, S. Bedoui, G. Molnar, A. Bousseksou, *Eur. Phys. J. Special Topics,* 2013, **222**, 1137-1159.

[44] M. Sy, F. Varret, K. Boukheddaden, G. Bouchez, J. Marrot, S. Kawata, S. Kaizaki, *Angew. Chem. Int. Ed.,* 2014, **53**, 7539-7542.

[45] C. Enachescu, M. Nishino, S. Miyashita, K. Boukheddaden, F. Varret, P. A. Rikvold, *Phys. Rev. B*, 2015, **91**, 104102.

[46] K. Yu. Maryunina, X. Zhang, S. Nishihara, K. Inoue, V. A. Morozov, G. V. Romanenko, V. I. Ovcharenko, *J. Mater. Chem. C*, 2015, **3**, 7788-7791.

[47] P. W. Anderson, P. R. Weiss, *Rev. Modern Phys*., 1953, **25**, 269-276.

[48] A. Carrington, A.D. McLachlan, Introduction to Magnetic Resonance with Applications to Chemistry and Chemical Physics, 1967.

[49] J. C. Bonner, M. E. Fischer, *Phys. Rev. A*, 1964, **135**, A640-A658.

[50] B. Silver, D. Getz, *J. Chem. Phys*., 1974, **61**, 638-650.

[51] C. J. Simmons, H. Stratemeier, G. R. Hanson, M. A. Hitchman, *Inorg. Chem*., 2005, **44**, 2753-2760.

[52] M. A. Hitchman, W. Maaskant, J. van der Plas, C. J. Simmons, H. Stratemeier, *J. Am. Chem. Soc*., 1999, **121**, 1488-1501.

[53] J. Goslar, M. Wencka, S. Lijewski and S. K. Hoffmann, *J. Phys. Chem. Solids*, 2006, **67**, 2614-2622.

[54] C. A. Kilner, E. J. L. McInnes, M. A. Leech, G. S. Beddard, J. A. K. Howard, F. E. Mabbs, D. Collison, A. J. Bridgeman, M. A. Halcrow, *Dalton Trans*., 2004, 236-243.

[55] S. Pillet, J. Hubsch, C. Lecomte, *Eur. Phys. J. B,* 2004, **38**, 541-552.

[56] P. Guionneau, S. Lakhloufi, M.-H. Lemée-Cailleau, G. Chastanet, P. Rosa, C. Mauriac, J.-F. Létard, *Chem. Phys. Lett.*, 2012, **542**, 52-55.

[57] P. Guionneau, *Dalton Trans*., 2014, **43**, 382-393.

TOC graphic

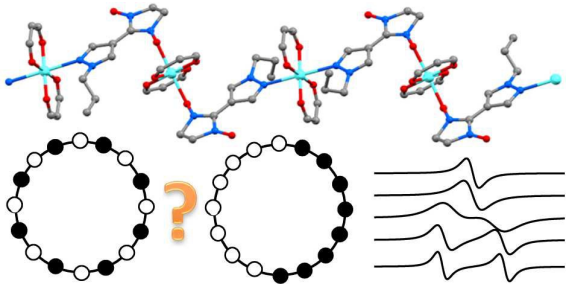

Thorough analysis of EPR and XRD data allows conclusions on spatial distribution of phases in copper-nitroxide molecular magnets

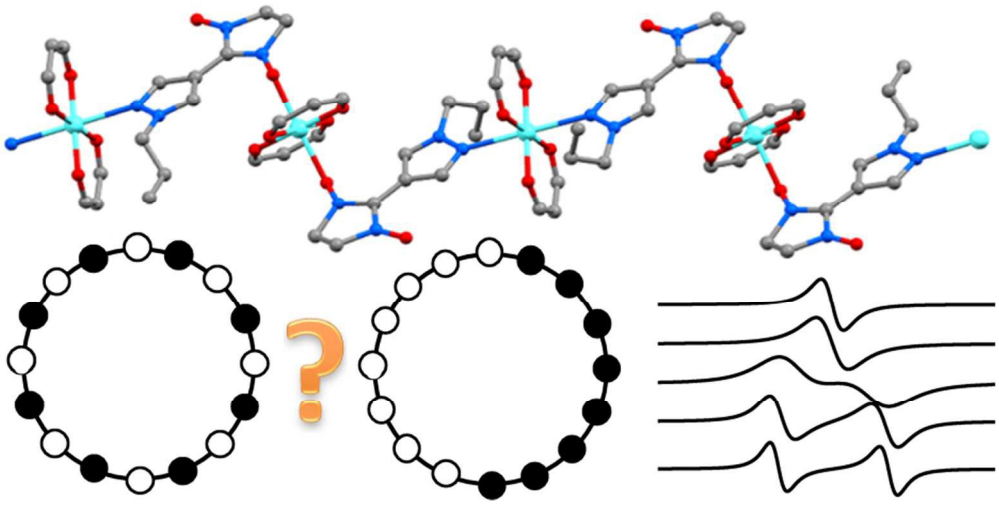

79x39mm (300 x 300 DPI)